RESEARCH ARTICLE | FEBRUARY 03 2014

Meyer-Neldel rule for Cu (I) diffusion in In_2S_3 layers

Albert Juma; Henry Wafula; Elke Wendler; Thomas Dittrich

Journal of Applied Physics 115, 053703 (2014)
https://doi.org/10.1063/1.4864125

Meyer-Neldel rule for Cu (I) diffusion in In_2S_3 layers

Albert Juma,[1,a)] Henry Wafula,[2] Elke Wendler,[3] and Thomas Dittrich[1]
[1]*Helmholtz-Zentrum Berlin für Materialien und Energie, Hahn-Meitner-Platz 1, 14109 Berlin, Germany*
[2]*Masinde Muliro University of Science and Technology, P.O. Box 190-50100, Kakamega, Kenya*
[3]*Institut für Festkörperphysik, Friedrich-Schiller-Universität Jena, Max-Wien-Platz 1, 07743 Jena, Germany*

(Received 14 January 2014; accepted 22 January 2014; published online 3 February 2014)

The nature of barriers for atomic transport in In_2S_3 layers has been varied by addition of chlorine. Diffusion of Cu(I) from a removable CuSCN source was used to probe the variation of the barriers. The Meyer-Neldel (compensation) rule was observed with a Meyer-Neldel energy (E_{MN}) and a proportionality prefactor (D_{00}) amounting to 40 meV and 5×10^{-14} cm^2/s, respectively. D_{00} shows that the elementary excitation step is independent of the specific mechanism and nature of the barrier including different densities of Cl in In_2S_3. The value of E_{MN} implies that coupling of the diffusing species to an optical-phonon bath is the source of the multiple excitations supplying the energy to overcome the diffusion barriers. © *2014 AIP Publishing LLC*.
[http://dx.doi.org/10.1063/1.4864125]

I. INTRODUCTION

The Meyer-Neldel (compensation) rule (MNR)[1] is a common property observed for a set of related activated processes in condensed matter physics,[1–4] chemistry,[5–7] geology,[8–10] and biology[11,12] that also satisfy the Arrhenius equation. In physics, MNR has been reported for electronic and atomic transport in atomic clusters, in the bulk and on surfaces, and for annealing, desorption and detrapping kinetics in both crystalline and amorphous materials.[13] MNR arises when the activation energy is large compared to both kT and the typical excitations of the system.[14–16] The amplitude of the prefactor to the exponential term in the Arrhenius equation increases exponentially when the activation energy increases leading to MNR. This rule is important for the analysis of transport phenomena including atomic diffusion.

According to the Eyring theory, the rate of a reaction is proportional to the exponential of the change in the free energy between the initial equilibrium position and the activated state.[17] The free energy is given by the difference between the activation enthalpy and entropy terms, where the enthalpy change is equivalent to the activation energy—the energy needed to overcome the barrier for the transition/reaction to take place. An increase in the activation energy results in a decrease of the exponential term in the Arrhenius expression but this decrease is compensated by an increase in the exponential prefactor resulting in the MNR.[1,13]

For transport processes such as atomic diffusion, the generation of the activation volume is likely to be due to multiphonon processes.[13,14] The larger the activation volume is, the more phonons will be required and the more paths there will be for the diffusing species to reach the activated state. This leads to the proportionality between the activation energy (E_A) and entropy (ΔS).[18] When E_A increases, the number of different ways for the diffusing species to reach the activated state, via multiphonon processes, also increases exponentially with E_A.[13–15] This is because the entropy is proportional to the logarithm of the number of ways of assembling the many excitations or multiphonon processes.[19,20]

Atomic diffusion is a thermally activated process that obeys the Arrhenius relation[16]

$$D(T) = D_{00} \cdot \exp\left(\frac{E_A}{E_{MN}}\right) \cdot \exp\left(-\frac{E_A}{k_B T}\right), \qquad (1)$$

where D is the diffusion coefficient, D_{00} and E_{MN} (so-called Meyer-Neldel energy) are constants independent of temperature, k_B is the Boltzmann constant, and T is the temperature in Kelvin scale. The value of E_{MN} is proportional to the characteristic energy of the heat bath or reservoir that supplies the energy needed for the transition of the diffusing species to the activated state.[14]

Different diffusion mechanisms are possible in solids depending upon the nature of the host material and the diffusing species. In most diffusion experiments, different diffusing species in the same matrix or the same diffusing species at different concentrations in matrices of different defect structure obey MNR.[21,22] For example, MNR has been observed for the diffusion of H at different H concentrations in a-Si:H (Ref. 23) and in a-Ge:H (Ref. 24) and for the diffusion of different elements in c-Si and KBr.[16]

The values of the MN energy for solids have been found to lie between 25 and 75 meV equivalent to typical optical-phonon energies (40–50 meV).[25] For example, experiments of annealing of various metastable defects in a-Si:H, doped and undoped, resulted in $E_{MN} = 40$ meV, while electronic experiments yielded values between 35 and 55 meV.[14] A study of the reverse saturation current from 23 different solar cells of 11 distinct categories with band gaps in the range of 1–2 eV resulted in an E_{MN} value of 31 meV.[26] Therefore, coupling to the optical-phonon bath is the possible source of the multiphonon excitations.[14]

Cationic vacancies in In_2S_3 crystals are crucial for Cu diffusion.[27] Two thirds of the introduced Cu occupies the cationic vacancies, while a third substitute for In in what is

a)Author to whom correspondence should be addressed. Electronic mail: albert.juma@helmholtz-berlin.de

termed insertion/substitution mechanism.[28] Layers of In_2S_3 are investigated as a model system in which the nature of barriers for transport has been varied by adding foreign atoms. In this sense, Cu (I) diffusion is used as a probe for the variation of the barriers in In_2S_3. The properties of In_2S_3 layers depend on the deposition method.[29] In this work, three classes of In_2S_3 layers based on deposition conditions are compared and they are (a) thermally evaporated In_2S_3,[30] (b) In_2S_3 deposited from indium acetylacetone ($In(acac)_3$) precursor salt by ion layer gas reaction (ILGAR)[31–33] leaving a small amount of residual carbon from the solvent, and (c) In_2S_3 deposited from $InCl_3$ precursor salt by ILGAR with varying amounts of Cl. The density of Cl was varied by changing the deposition parameters in the ILGAR deposition process.[33] CuSCN was used as a removable source for Cu(I).[30]

Rutherford backscattering spectrometry (RBS) was used for the analysis of the depth dependent densities of constituent elements (In, S, Cu, and Cl) after diffusion experiments.[34] The diffusion coefficients of Cu(I) were obtained from the analysis of the depth profiles.

II. EXPERIMENTS

Thermally evaporated In_2S_3 layers, hereafter called In_2S_3 (PVD), were treated in Ref. 30; therefore, the results from this reference will be used along with similarly treated samples as described in this section. The In_2S_3 layers were deposited on c-Si substrates of about 1 in. diameter. A set of samples were deposited by spray-ILGAR from 25 mM solution of $In(acac)_3$ or $InCl_3$ precursor salt dissolved in ethanol.[31,32] The spray-ILGAR deposition process is sequential and involves spraying the precursor solution sulfurization by exposure of the precursor layer to H_2S gas with pauses in between.[33] These steps were modified to produce In_2S_3 layers with varying Cl content. In_2S_3 layers from $In(acac)_3$ precursor are herein named In_2S_3(acac), while layers from $InCl_3$ precursor are termed In_2S_3(Cl). The flow rate of the H_2S gas was 0.0375 or 0.95 l per minute for the 100% or 5% concentrations, respectively.

As an inexhaustible Cu(I) source, CuSCN was deposited onto the c-Si/In_2S_3 samples from a solution of 0.05 M CuSCN in propyl sulfide[35] using spray-spin method.[30] Ten spray-spin cycles of the solution were deposited to produce layers of about 500 nm thick. Each c-Si/In_2S_3/CuSCN sample was cut into several smaller pieces. The diffusion experiments were performed by annealing the small pieces of c-Si/In_2S_3/CuSCN from the two sets of samples on a hot plate in air at ambient pressure and at temperatures of 150, 175, 200, 225, and 250 °C for 5 min each. One bare c-Si/In_2S_3 and one as-deposited c-Si/In_2S_3/CuSCN sample from each set was left without annealing to serve as a reference. The CuSCN layers were removed from all the samples by dipping in pyridine solution, rinsing in de-ionized water, and drying in a flow of nitrogen gas, leaving behind c-Si/In_2S_3:Cu layers.[30] RBS experiments were performed on bare c-Si/In_2S_3 and c-Si/In_2S_3:Cu layers using a He^+ ion beam of energy 1.44 MeV. The scattering angle was 168° and the charge 10 μC. The bare c-Si/In_2S_3 samples were used to determine the stoichiometry and initial thickness of the layers.

III. DEPTH PROFILING AND DETERMINATION OF DIFFUSION COEFFICIENTS

An example of the RBS spectra from In_2S_3(Cl) is shown in Fig. 1. The RBS signals from Si, S, Cl, Cu, and In are indicated. The relative position of a RBS signal is determined by the atomic mass of the respective element detected in the sample. The RBS signals from the light Si atoms of the substrate appear at the lowest channel numbers, i.e., at the lowest energy. The S and Cl signals overlapped partially due to the relatively small difference in their atomic masses. The thickness of the In_2S_3 layers was chosen in such a way that there was no overlap of the RBS signals related to Cu and In. The signal from Cu increased with increasing annealing temperature due to enhanced Cu diffusion from the CuSCN source layer into the In_2S_3 layer.

Figure 2 shows the parts of the RBS spectra from Cu for In_2S_3(acac) (a) and In_2S_3(Cl) (b) layers. The height of the signals decreased towards lower channel numbers, which signifies a decrease in the Cu concentration in In_2S_3:Cu layers with depth from the surface. The high RBS signal between channels 380 and 390 in all samples is a signature of a thin surface layer with a high concentration of Cu. The rate of increase of the Cu signal with annealing temperature for In_2S_3(Cl) was relatively slower than that for In_2S_3(acac). The residual Cl tends to limit the diffusion and distribution of Cu in the In_2S_3 matrix.

The depth profiles of diffused Cu in In_2S_3:Cu layers were extracted from the RBS spectra using Nuno's Data Furnace (NDF) code,[34,36] which calculates the RBS spectra from experimental parameters and compares with the measured spectra. The In_2S_3 layers were subdivided into thin sub-layers and the elemental concentrations of each sub-layer adjusted as the spectra were calculated using experimental parameters until the best fit was achieved. The elemental compositions

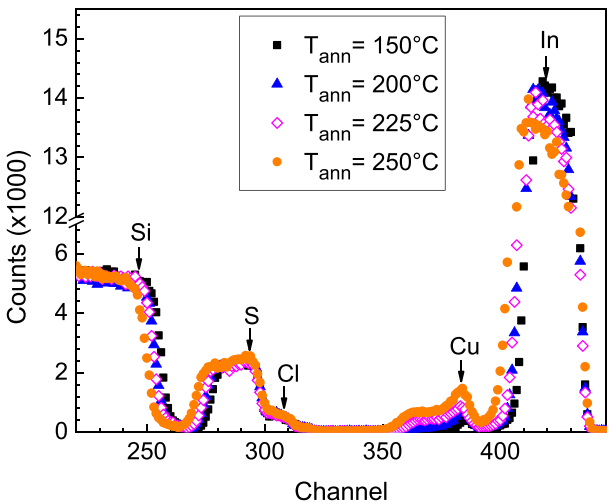

FIG. 1. RBS spectra for sample (c) (In_2S_3:Cu layers) after diffusion of Cu (I) at temperatures of 150 (squares), 175 (closed circles), 200 (triangles), 225 (open diamonds), and 250 °C (open circles). The signals from Si, S, Cl, Cu, and In are indicated.

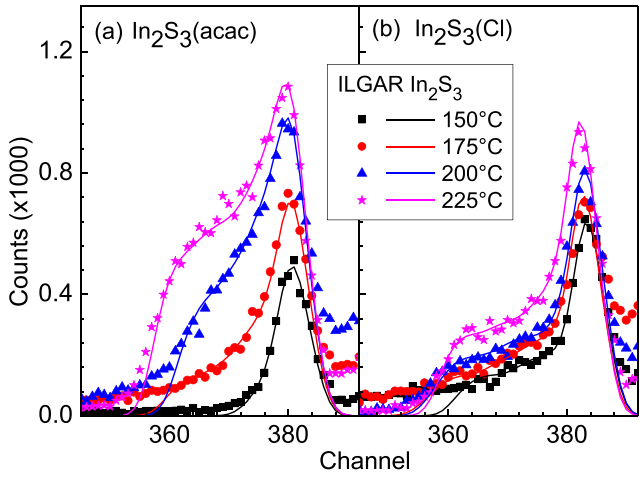

FIG. 2. RBS signal from diffused Cu in evaporated In_2S_3 (a) and In_2S_3 layers deposited from $In(acac)_3$ (b) or $InCl_3$ (c) precursor, after annealing at temperatures of 150 (squares), 175 (circles), 200 (triangles), and 225 °C (stars). The symbols and lines represent the measured data and simulated spectra, respectively.

and the thicknesses of the sub-layers gave the depth distributions of each element. In Figure 2, the symbols represent the measured data, while the continuous lines are the simulated spectra.

The concentration of Cu versus depth resulting from the RBS analysis is plotted in Figure 3 for (a) In_2S_3(acac) and (b) In_2S_3(Cl). It was found that a thin surface layer of about 6-8 nm thick with a high density of Cu, independent of the annealing temperature, existed in all samples. This was due to the formation of an interfacial layer after annealing between CuSCN and In_2S_3 as reported also for Cu(In,Ga)Se_2/In_2S_3 interfaces.[37,38] To obtain values for the diffusion coefficients (D_{Cu}) for the different In_2S_3:Cu layers and for different annealing temperatures, a one dimensional diffusion model for simulating the depth profiles by numerically solving Fick's second law of diffusion was implemented.[30] The values of D_{Cu} were first approximated by fitting the measured Cu profiles with an error function and then using the values of D_{Cu} giving the best fit as the starting values for the simulation of the depth profiles using a recursion expression.

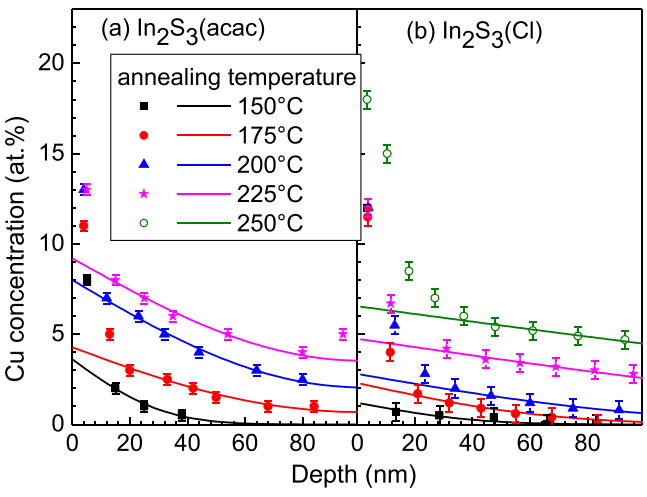

FIG. 3. Depth profiles of diffused Cu in evaporated In_2S_3 (a) and In_2S_3 layers deposited from $In(acac)_3$ (b) or $InCl_3$ (c) precursor, after annealing at temperatures of 150 (squares), 175 (circles), 200 (triangles), 225 °C (stars), and 250 °C (open circles). The symbols and lines represent the measured data and simulated profiles, respectively.

The simulation parameters were adjusted until the simulated profiles reproduced the measured data with minimum deviation. The high Cu density at the surface was not taken into account because the Cu density was independent of the annealing temperature. The measured (symbols) and simulated (solid lines) depth profiles of Cu in In_2S_3(acac) and In_2S_3(Cl) layers after annealing at temperatures of 150, 175, 200, 225, and 250 °C and removal of CuSCN are plotted in Figure 3. The depth profiles could be fitted each with one diffusion coefficient, signifying one diffusion mechanism of Cu migration in all the In_2S_3 host layers. It can be remarked that the thickness of the surface layer with high Cu density increased at temperatures above 225 °C, especially for In_2S_3(Cl) layers as seen in Figure 3(b).

For In_2S_3(PVD) layers, the values of D_{Cu} at annealing temperatures of 175, 200, 225, and 250 °C amounted to 3.1×10^{-14}, 4.3×10^{-14}, 8.0×10^{-14}, and 8.8×10^{-14} cm^2/s, respectively (taken from Ref. 30). For In_2S_3(acac) layers, the values of D_{Cu} at annealing temperatures of 150, 175, 200, 225, and 250 °C were 1.0×10^{-14}, 5.5×10^{-14}, 7.4×10^{-14}, 1.0×10^{-13}, and 1.4×10^{-13} cm^2/s, respectively, and as an example for In_2S_3(Cl = 8.5 at. %) layers D_{Cu} values amounted to 1.8×10^{-14}, 4.7×10^{-14}, 1.1×10^{-13}, 4.4×10^{-13}, and 9.9×10^{-13} cm^2/s, respectively.

IV. DIFFUSION MECHANISMS AND THE MEYER-NELDEL RULE

Figure 4 shows the Arrhenius plots of D_{Cu} in In_2S_3(acac) and In_2S_3(Cl) layers as a function of the inverse of the annealing temperature. The activation energies (E_A) and diffusion prefactors (D_0) for Cu diffusion in Cl-free and in Cl-containing In_2S_3 layers were obtained by fitting the diffusion coefficient curves with the Arrhenius equation (1).

There is no systematic change of either D_0 or E_A with corresponding change in Cl density. The activation energies for the Cl-free samples In_2S_3(acac) and In_2S_3(PVD) amounted to 0.24 and 0.30 eV, respectively, and were more than two times lower than those for the In_2S_3(Cl) samples.

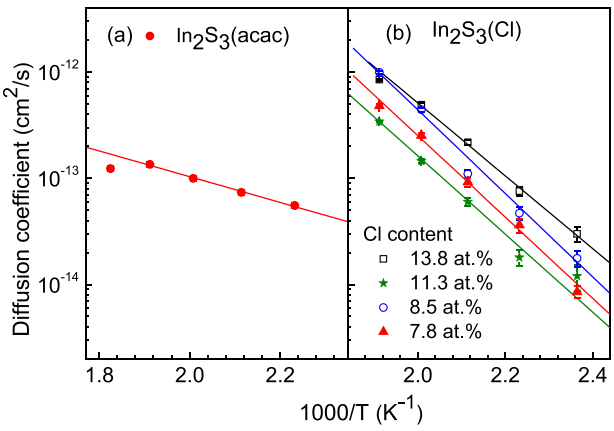

FIG. 4. Arrhenius plot of diffusion coefficients of Cu against temperature in evaporated-In_2S_3 and In_2S_3 layers deposited from $In(acac)_3$ or $InCl_3$ precursors with varying Cl amounts.

The values of E_A for Cu diffusion in In_2S_3(Cl) layers were 0.76, 0.78, 0.72, and 0.70 eV corresponding to residual Cl densities of 7.8, 8.5, 11.3, and 13.8 at. %, respectively. Increasing the Cl density by a factor of two (from 7.8 to 13.8 at. %) did not change the activation energy significantly. The values of D_0 for the Cl-free samples In_2S_3(acac) and In_2S_3(PVD) were of the same magnitude but almost five orders of magnitude smaller than for the Cl-containing samples. The increase in the D_0 follows due to an increase in the activation entropy (ΔS).[18–20]

The stoichiometry of the In_2S_3 layers was obtained from the ratios of the concentrations of the constituent elements in each of the In_2S_3 layers. The Cl-free layers were more stoichiometric, with the deviation from stoichiometry increasing with the amount of residual Cl. The ratio of [S]/[In] for as-deposited In_2S_3(PVD) and In_2S_3(acac) layers amounted to 1.53 and 1.56, respectively, showing S excess. The ratio [S]/[In] for as-deposited In_2S_3(Cl) layers was 1.44, 1.43, 1.39, and 1.32 corresponding to Cl concentrations of 7.8, 8.5, 11.3, and 13.8 at. %, respectively. The general chemical formula was derived as $In_4S_{6-2x}Cl_{2x+2y}$. The subscripts x and y represent the residual Cl bonded to In and the excess Cl found in the In_2S_3 matrix, which may occupy interstitial position or cationic vacancies as antisites.

The residual Cl in the In_2S_3 matrix changes the local bond configurations that can limit the migration of Cu in In_2S_3(Cl) compared to stoichiometric In_2S_3 layers. It is known that Cu diffuses in In_2S_3 via vacancy[27] and/or insertion and substitution mechanism.[28] The presence of Cl decreases the density of available vacancies in In_2S_3 and, therefore, limits diffusion by the vacancy mechanism. The In-Cl bond limits the substitution of In by Cu because of the relatively stronger In-Cl bond (428 KJ/mol) compared to Cu-S (275 KJ/mol) or In-S (288 KJ/mol) bonds.[39] This increases the barrier for Cu diffusion in In_2S_3(Cl).

The activation energy of atomic diffusion is influenced by the nature of bonding in the host material.[40] This explains the observed increase in the activation energy with incorporation of Cl in the In_2S_3 matrix. The change in bonding due to residual Cl also increases the band gap,[32] decreases the work function,[41] and improves the photosensitivity[42] of In_2S_3 layers. Surface photovoltage (SPV) experiments[41] have also shown a significant reduction in the degree of disorder in In_2S_3(Cl) compared to In_2S_3(acac) layers. These changes in the electronic properties affect the chemical potential of In_2S_3, which impacts on the exponential prefactor.

Figure 5 shows a plot of the natural logarithm of the diffusion prefactor (ln D_0) against the activation energy in a Meyer-Neldel plot. Copper diffusion in In_2S_3 layers of different stoichiometry satisfies the MNR. The Meyer-Neldel energy (E_{MN}) was obtained from the slope of the graph by fitting the data with Eq. (2) and amounted to 40 meV. This is equivalent to the value obtained for annealing processes in a-Si:H.[14] The characteristic temperature $T_0 = E_{MN}/k_B = 191\,^{\circ}C$. The value of T_0 is related to the average of the temperature range covered in this work,[21] which is 200 °C. The value of $D_{00} = 5 \times 10^{-14}$ cm^2/s defines the diffusion coefficient at T_0. The value of E_{MN} is on the order of the energy of the excitations permitting the activation, while D_{00} shows that the elementary excitation steps are independent of the specific mechanism.[13]

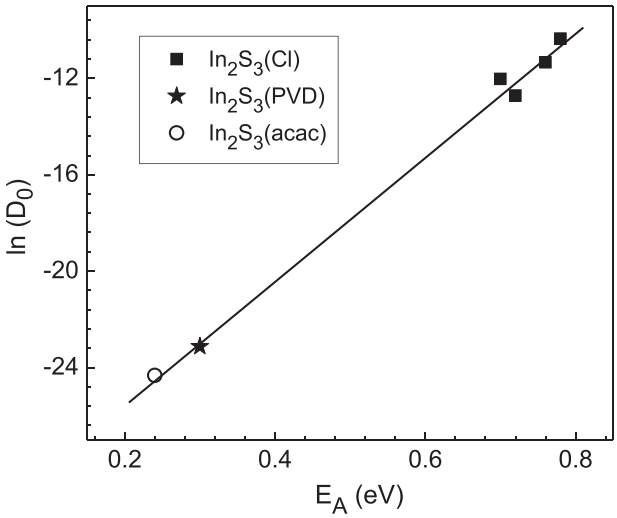

FIG. 5. Natural logarithm of the diffusion prefactor (D_0) as a function of the activation energy (E_A) for Cu diffusion in different In_2S_3 layers. The values for In_2S_3 (PVD) have been taken from Ref. 30.

The MNR arises from the fact that the source of the energy and the mechanisms of energy transfer for the atomic transitions are the same.[14,15] Semiconductors with band gaps of 1–2 eV (In_2S_3 has a band gap of 2.0 eV) will therefore have E_{MN} values in this range because they obtain their excitation energy from baths, and through interactions, with similar characteristics (Ref. 13 and references therein). From the value of E_{MN}, it can be concluded that coupling of the diffusing Cu to an optical-phonon bath is the source of the multiple excitations supplying the energy to overcome the diffusion barriers in In_2S_3.[14]

V. CONCLUSION

We have shown the role of residual Cl, and therefore, the role of foreign atoms in a host material, for Cu(I) diffusion in In_2S_3 layers. Residual Cl modifies the local bond configuration in In_2S_3(Cl) as well as the diffusion mechanisms resulting in an increase in the activation energy. The MNR holds when the activation entropy is proportional to the activation energy, which accounts for the increase in the exponential prefactor with corresponding increase in the activation energy. The Meyer-Neldel energy of 40 meV agrees well with values obtained from activated processes in other materials of similar band gap. This means that the excitation energy and interactions are from reservoirs with similar characteristics.

ACKNOWLEDGMENTS

A.J. and H.W. appreciate financial support from DAAD. The authors appreciate the technical support of Mr. Barth in RBS measurements, N. Barreau for constructive discussion on diffusion mechanisms, and Ch.-H. Fischer and R. Sáez-Araoz for introduction to ILGAR.

[1]W. Meyer and H. Neldel, Z. Tech. Phys. **12**, 589 (1937).
[2]V. P. Zhdanov, Surf. Sci. Rep. **12**, 185 (1991).

[3]J. A. M. Abu Shama, S. W. Johnson, R. S. Crandall, and R. Noufi, Appl. Phys. Lett. **87**, 123502 (2005).
[4]T. A. Abtew, M. Zhang, Y. Pan, and D. A. Drabold, J. Non-Cryst. Solids **354**, 2909 (2008).
[5]E. L. Kapinus and H. Rau, J. Phys. Chem. A **102**, 5569 (1998).
[6]W. Linert and R. F. Jameson, Chem. Soc. Rev. **18**, 477 (1989).
[7]D. De Marco and W. Linert, J. Chem. Thermodyn. **34**, 1137 (2002).
[8]S. R. Hart, Geochim. Cosmochim. Acta **45**, 279 (1981).
[9]S. M. Fortier and B. J. Giletti, Geochim. Chem. Cosmochim. Acta **55**, 1319 (1991).
[10]R. W. Keyes, J. Chem. Phys. **29**, 467 (1958).
[11]B. Rosenberg, B. B. Bhowmik, H. C. Harder, and E. Postow, J. Chem. Phys. **49**, 4108 (1968).
[12]B. Rosenberg, G. Kemeny, R. C. Switzer, and T. C. Hamilton, Nature **232**, 471 (1971).
[13]A. Yelon, B. Movaghar, and R. S. Crandall, Rep. Prog. Res. **69**, 1145 (2006).
[14]A. Yelon, B. Movaghar, and H. Branz, Phys. Rev. B **46**, 12244 (1992).
[15]A. Yelon and B. Movaghar, Phys. Rev. Lett. **65**, 618–620 (1990).
[16]K. Shimakawa and A. Aniya, Monatsh. Chem. **144**, 67 (2013).
[17]H. Eyring, J. Chem. Phys. **3**, 107 (1935).
[18]A. W. Lawson, J. Chem. Phys. **32**, 131 (1960).
[19]G. Boisvert, N. Mousseau, and L. J. Lewis, Phys. Rev. B **58**, 12667 (1998).
[20]G. Boisvert, L. J. Lewis, and A. Yelon, Phys. Rev. Lett. **75**, 469 (1995).
[21]R. Kirchheim and X. Huang, Phys. Status Solidi B **144**, 253 (1987).
[22]C. Wert and C. Zener, Phys. Rev. **76**, 1169 (1949).
[23]J. Shinar, R. Shinar, X.-L. Wu, S. Mitra, and R. F. Girvan, Phys. Rev. B **43**, 1631 (1991).
[24]X.-L. Wu, J. Shinar, and R. Shinar, Phys. Rev. B **44**, 6161 (1991).
[25]A. Yelon and B. Movaghar, Phys. Rev. B **65**, 077202 (2002).
[26]T. J. Coutts and N. M. Pearsall, Appl. Phys. Lett. **44**, 134 (1984).
[27]F. Py, M. Womes, J. M. Durand, J. Olivier-Fourcade, S. C. Jumas, J. M. Estera, and R. C. Karnatak, J. Alloys Compd. **178**, 297 (1992).
[28]C. Guillot-Deudon, S. Harel, A. Mokrani, A. Lafond, N. Barreau, V. Fernandez, and J. Kessler, Phys. Rev. B **78**, 235201 (2008).
[29]N. Bareau, Sol. Energy **83**, 363 (2009).
[30]A. O. Juma, P. Pistor, S. Fengler, Th. Dittrich, and E. Wendler, Thin Solid Films **520**, 6740 (2012).
[31]J. Moeller, Ch.-H. Fischer, H.-J. Muffler, R. Konenkamp, I. Kaiser, C. Kelch, and M. C. Lux-Steiner, Thin Solid Films **361–362**, 113 (2000).
[32]H.-J. Muffler, Ch.-H. Fischer, K. Diesner, and M. C. Lux-steiner, Sol. Energy Mater. Sol. Cells **67**, 121 (2001).
[33]R. Sáez-Araoz, J. Krammer, S. Harndt, T. Koehler, M. Krueger, P. Pistor, A. Jasanek, F. Hergert, M. C. H. Lux-Steiner, and Ch.-H. Fischer, Prog. Photovoltaics **20**, 855 (2012).
[34]C. Jeynes, N. P. Barradas, H. Rafla-Yuan, B. P. Hichwa, and R. Close, Surf. Interface Anal. **30**, 237 (2000).
[35]G. R. R. A. Kumara, A. Konno, G. K. R. Sanedeera, P. V. V. Jayaweera, D. B. R. A. De Silva, and K. Tenakona, Sol. Energy Mater. Sol. Cells **69**, 195 (2001).
[36]N. P. Barradas, C. Jeynes, and R. P. Webb, Appl. Phys. Lett. **71**, 291 (1997).
[37]D. Abou-Ras, G. Kostorz, A. Strohm, H. W. Schock, and A. N. Tiwari, J. Appl. Phys. **98**, 123512 (2005).
[38]D. Abou-Ras, D. Rudmann, G. Kostorz, S. Spiering, M. Powalla, and A. N. Tiwari, J. Appl. Phys. **97**, 084908 (2005).
[39]Y.-R. Luo, *Comprehensive Handbook of Chemical Bond Energies* (CRC Press, 2007).
[40]B. I. Boltak, *Diffusion in Semiconductors* (Infosearch Ltd, London, 1963).
[41]A. Juma, A. Azarpira, A. Steigert, M. Pomaska, Ch.-H. Fischer, I. Lauermann, and Th. Dittrich, J. Appl. Phys. **114**, 053711 (2013).
[42]A. Cherian, M. Mathew, C. Kartha, and K. Viyajakamar, Thin Solid Films **518**, 1779 (2010).